Science Advances Today

Sci. Adv. Today 2 (2016) 25243

EPR and magnetic studies of sub-microcrystalline pure and Yb doped $Na_3B(PO_4)_2$ (B=Y, La, Gd) orthophosphates synthesized by hydrothermal and Pechini method

S. M. Kaczmarek[a], G. Leniec[a], H. Fuks[a], T. Skibiński[a], A. Pelczarska[b], I. Szczygieł[b], J. Hanuza[b,c]

[a] Institute of Physics, West-Pomeranian University of Technology, Al. Piastów 17, 70-311 Szczecin, Poland
[b] Faculty of Chemistry and Food Technology, Wrocław University of Economics, ul. Komandorska 118/120, 53-345 Wrocław, Poland
[c] Institute of Low Temperature and Structure Research, Polish Academy of Sciences, ul. Okólna 2, 50-422 Wrocław, Poland

[*]Author for correspondence: S. M. Kaczmarek, email: smkaczmar@wp.pl
Received 28 Jun 2016, Accepted 29 Aug 2016, Published Online 29 Aug 2016

The EPR properties and magnetic susceptibility of pure and Yb^{3+} ion doped sodium rare-earths element double orthophosphates were investigated. The magnetic properties of the compounds obtained by hydrothermal and Pechini methods were compared. Their calcination at tempeartures: 120°C, 500°C, 700°C and 1100°C was carried out in order to describe phase structures evolving with increasing calcination temperature. EPR analysis allowed us to find clear differences between the gadolinium ions arrangement in undoped and doped with ytterbium $Na_3Gd(PO_4)_2$, obtained by hydrothermal and Pechini methods. It was possible by finding spin-Hamiltonian parameters calculated for some pure and ytterbium doped orthophosphates.

1. INTRODUCTION

Rare-earths element phosphates and their combinations with alkali metals/ alkaline earth metals exhibit good chemical and thermal stability, optical efficiency and can be prospective laser and magnetic materials. The studied host materials belong to the family of double phosphates of mono- and trivalent cations with the formula $M^I_3M^{III}(PO_4)_2$ (M^I = Na, K; M^{III} = Y, Sc, In, Fe, RE – rare earths element) [1-3]. The structure of the phosphates in all phases consists of separated PO_4 tetrahedra and Na^+ and RE^{3+} ions lying among them. In Scheme 1 the atomic arrangement of $Na_3Gd(PO_4)_2$ is shown as an example of analyzed orthophosphates. The sodium-rare earths double orthophosphates reveal structural phase transitions. It is well known [1-4] that bulk crystals of orthophosphates with M^{III} ion from Gd to Er exhibit a sequence of phase transitions from monoclinic at low temperature, to orthorhombic and trigonal at high temperature (generally above about 1000 °C). Sodium gadolinium phosphate, $Na_3Gd(PO_4)_2$, crystallizes in various crystal structures: trigonal, tetragonal, orthorhombic [5] and monoclinic [6]. The trigonal phase is characterized by statistical occupation of the same position by Na and RE. In this phase RE^{3+} ions occupy the sites of the C_1 general symmetry, and they can be substituted by doping ions. The orthorhombic phase is characterized by space groups $Pca2_1$ (C_{2v}^5, No. 29, Z = 8) and the unit cell parameters of about $a \approx 13.9$, $b \approx 5.3$ and $c \approx 18.3$ Å, V = 1367 Å^3 [6]. The structure of the monoclinic modification was refined in the space group C2/c (C_{2h}^6, No. 15, Z=12) with the unit cell parameters of about: a = 13.9, b = 5.5, c = 27.5 Å, β = 91.3°, V = 2039 Å^3 [5]. Calcination of the studied phosphates at, e.g. 500 and 700 °C changes their microstructure as well as the sample composition.

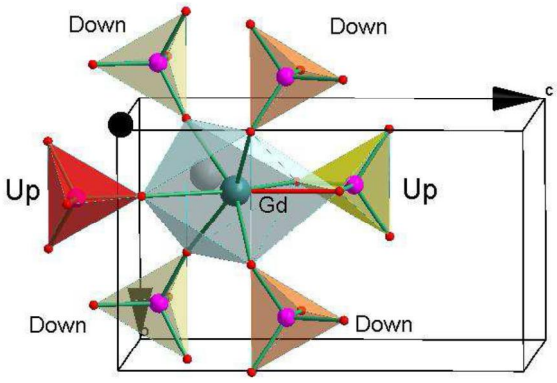

Scheme 1. $Na_3Gd(PO_4)_2$ – atomic arrangement.

Table 1. Some types of magnetic interactions appearing as spin Hamiltonian terms [9].

Components of the Hamiltonian	
Electronic Zeeman term	$H_{Zeeman} = \mu_B \mathbf{g}_e \mathbf{B} \cdot \mathbf{S}$
Nuclear Zeeman term	$H_{Zeeman} = \mu_B \mathbf{g}_n \mathbf{B} \cdot \mathbf{I}$
Zero Field Splitting (ZFS) term	$H_{ZFS} = \mathbf{S} \cdot \mathbf{D} \cdot \mathbf{S}$
	$H_{ZFS} = D\left[S_z^2 - \frac{1}{3}S(S+1)\right] + E\left(S_x^2 - S_y^2\right)$ D – axial and E – rhombic distortions of octahedral
Dipole-dipole interaction	$H_{pair} = \mathbf{S}^A \cdot \mathbf{D}_{dd}^{AB} \cdot \mathbf{S}^B$
High term (Stevens notation)	$H = \sum_{m=-l}^{l} \mathbf{B}_l^m \cdot \mathbf{O}_l^m(\mathbf{S})$
Hyperfine interaction	$H = \mathbf{S} \cdot \mathbf{A} \cdot \mathbf{I}$
Quadrupole interaction	$H = \mathbf{I} \cdot \mathbf{P} \cdot \mathbf{I}$

Nano- and microcrystalline phosphates can be used as a starting material in manufacturing of transparent ceramics that ensure required optical properties and preserve –single crystal form. Yttrium, lanthanum and gadolinium sodium-orthophosphates doped with Yb^{3+} ions were studied in [7], where Pechini method was used for synthesis of submicro-sized samples. It was reported that the Pechini method used in the synthesis of $Na_3RE(PO_4)_2$ type orthophosphate (*RE* = Y, La, Gd) allowed to obtain the orthorhombic $Pca2_1 = C_{2v}^5$ structure for $Na_3La(PO_4)_2$ and $Na_3Gd(PO_4)_2$ powders and the monoclinic $C2/c = C_{2h}^6$ structure for $Na_3Y(PO_4)_2$. All these compounds showed structural transformations at high temperature. The powders calcined at 700 °C were built of the particles ca. 0.7 – 3 μm in size forming agglomerates whose shape depended on RE^{3+} ion type. Particles of La compound formed irregular agglomerates, while Gd ones were characterized by spherical agglomerates of about 3 μm size. $Na_3Y(PO_4)_2$ crystals formed plate–like agglomerates of 1.5 x 2 μm size. Annealing of these orthophosphates at 1100°C induced an intense growth of grains up to about 4 μm. It was also found that the Pechini method gave the final product in the form of agglomerates the quantum efficiency of which was weak. Thus, the obtained by this method phosphates could not be used as efficient optical materials.

On the other hand, the hydrothermal method used to synthesise $Na_3Y(PO_4)_2$ and $Na_3Gd(PO_4)_2$ orthophosphates allowed to obtain their trigonal modifications (for the as-synthesized samples), and orthorhombic or monoclinic modifications after calcination of the as-synthesized samples at 500 or 700°C [8]. The shape of the particles formed by precipitation under hydrothermal conditions resembles rice grains. It means, that the grain size, morphology and spectroscopic properties of the studied phosphates crucially depend on the method of preparation. It was reported that the hydrothermal synthesis is a suitable method for obtaining a prospective material for optical applications, on the contrary to those synthesized by Pechini method [8].

An analysis of magnetic properties and local environment of different RE dopants in the compounds by using EPR technique may be performed by at least two ways. The first one is an analysis of the EPR lineshape and the second one is an analysis of temperature and angular dependences of the EPR signal. In the case of a single crystal both ways are more clear due to sharp signals. In the case of powders or nanopowders the signals are broaden and require another approach. The spin-Hamiltonian can describe different types of magnetic interactions in materials; they are shown in Table 1.

By analyzing spin-Hamiltonian parameters of a higher order (Steven's parameters different from zero) some features of the local symmetry of the analyzed ions can be described. Some relations between crystal and local symmetries and dependences between spin-Hamiltonian parameters are presented in Table 2.

In this work we describe the EPR properties of pure and ytterbium doped gadolinium, yttrium and lantanium sodium-orthophosphates obtained by hydrothermal and Pechini syntheses.

2. MATERIALS AND METHODS

$Na_3Gd(PO_4)_2$ (NGP) orthophosphates pure and doped intentionally by 5% of Yb, were prepared by hydrothermal technique using Magnum II autoclave (Ertec, Poland). The details of this process was described elsewhere [8]. The synthesis was carried out for 1 h at maximal temperature of 240°C (513 K) and pressure of about 25 atm. As-obtained fine precipitates were centrifuged, washed several times with distilled water and dried at 120 °C (393 K). Finally, these precursors were calcined at 500°C (773 K) or 700°C (973 K) for 10 h. The shape of the studied material particles resembled rice grains. Their size was ca. 0.7×2 μm and 0.33 × 1.5 μm for the precursor samples and those calcined at 700°C, respectively. The grain size of the synthesized by Pechini method powders was significantly larger, ca. 3 μm for the former and ca. 1.5 × 2 μm for the latter compound. The shape of the grains obtained by Pechini method was spherical [8]. The investigated samples were marked as: NGP 120, NGP 500 and NGP 700 in the case of pure orthophosphates and NGPYb 120, NGPYb 500 and NGPYb 700 in the case of the samples doped with Yb^{3+}. A temperature without a name of compound is calcination temperature, Yb 5% means intentional doping of the compounds with ytterbium.

The second set of samples, $Na_3Gd(PO_4)_2$: 5% Yb orthophosphates, was prepared by modified Pechini method [7]. Following rare earths oxides were used in the synthesis: Yb_2O_3 (99.9%, Aldrich, Germany) and Gd_2O_3 (99.9% Kare, England). At first, about 0.5 g of the oxides were digested in 4 ml of concentrated HNO_3 (analytically pure, POCh). At the synthesis stage doping with ytterbium was also performed by digestion of a stoichiometric mixture of Gd_2O_3 and Yb_2O_3 in nitric acid. The obtained solutions were diluted with a small amount of distilled water, next citric acid (CA) and ethylene glycol (EG) were added. Both chemicals were used in the Gd:CA:EG =1:5:5 molar ratio. The obtained solutions were heated under mixing until they became viscous. Then, stoichiometric amounts of $NH_4H_2PO_4$ and $Na_3PO_4 \cdot 12\ H_2O$ were added. The solutions were further heated until foamed gels were obtained. The resulted gels were dried for 20 h at 80°C and for 40 h at 120°C. Finally, individual samples were calcined at 700°C and 1100°C for 10 h. The investigated samples were marked similarly as hydrothermal samples: NGPYb 700 and NGPYb 1100.

Table. 2. Crystal symmetry and parameters of spin Hamiltonian, S=5/2 [10, 11].

Crystal family/crystal system	Schöenflies notation (EPR-NMR)	Hamiltonian values
Triclinic (lowest)	C_1; C_i=S_2	$gx \neq gy \neq gz$ $\alpha \neq \beta \neq \gamma \neq 90^0$ $B_2^0, B_2^2, B_4^0, B_4^1, B_4^{-1},$ $B_4^2, B_4^{-2}, B_4^3, B_4^{-3}, B_4^4, B_4^{-4}$
Monoclinic	C_2; C_s=C_{1h}; C_{2h}	$gx \neq gy \neq gz$ $\alpha = \beta = 90^0, \gamma \neq 90^0$ $B_2^0, B_2^2, B_4^0, B_4^2, B_4^{-2}, B_4^4, B_4^{-4}$
Orthorombic	D_2=V; C_{2v}; D_{2h}	$gx \neq gy \neq gz$ $\alpha = \beta = \gamma = 90^0$ $B_2^0, B_2^2, B_4^0, B_4^2, B_4^4$
Tetragonal	C_4; S_4; C_{4h}; D_4; C_{4v}; D_{2d}; D_{4h}	$gx = gy \neq gz$ $\alpha = \beta = \gamma = 90^0$ B_2^0, B_4^0, B_4^4
Hexagonal/Trigonal	C_3; S_6=C_{3i}; D_3; C_{3v}; D_{3d}	$gx = gy = gz$ $\alpha = \beta = \gamma \neq 90^0$ B_2^0, B_4^0, B_4^3
Hexagonal/Hexagonal	C_6; C_{3h}; C_{6h}; D_6; C_{6v}; D_{3h}; D_{6h}	$gx = gy \neq gz$ $\alpha = \beta = 90^0, \gamma = 120^0$ B_2^0, B_4^0
Cubic (highest)	T; T_h; O; T_d; O_h	$gx = gy = gz$ $\alpha = \beta = \gamma = 90^0$ $a/120 = B_4^0 + 5B_4^4$ $a/120 = B_4^0 + 20\sqrt{2}B_4^3$

Besides gadolinium orthophosphates we also analyzed yttrium (NYPYb 120, NYPYb 500 and NYPYb 700) orthophosphates doped with Yb (obtained by hydrothermal method) and yttrium (NYPYb 700) and lanthanum (NLPYb 700 and NLPYb 1150) orthophosphates doped with ytterbium (obtained by Pechini method), to make resolution of ytterbium EPR spectra clear, they are not recognizable in gadolinium orthophosphates.

The first derivative of the absorption spectrum was recorded as a function of the applied magnetic field using a conventional X-band Bruker ELEXSYS E 500 CW-spectrometer operating at 9.5 GHz with 100 kHz magnetic field's modulation. Temperature dependences of EPR spectra of the samples in the temperature range 3-300 K using an Oxford Instruments ESP helium-flow cryostat and in the temperature range 78-300 K using an Oxford Instruments ESP nitrogen-flow cryostat were recorded. The two types of cooling media were used to confirm small changes in the resonance line positions detected with higher (helium) and lower (nitrogen) damping of EPR signal. EPR/NMR program was used to find the local symmetry and spin-Hamiltonian parameters of gadolinium and ytterbium ions [11].

Static (dc) magnetic susceptibility measurements were performed using a Quantum Design MPMS XL-7 with EverCool Magnetic Property Measurement System at temperature from 4 K up to 305 K and magnetic fields of 1000–10,000 Oe. Dc susceptibilities were measured in the zero-field-cooling (ZFC) and field-cooling (FC) modes.

3. RESULTS

3.1. $Na_3Gd(PO_4)_2$ powder samples obtained by hydrothermal method

Powder samples of the $Na_3Gd(PO_4)_2$ powder, obtained by hydrothermal method, marked as NGP 120, NGP 500 and NGP 700 (calcined at temperature: 120, 500 and 700°C for 10 h) were investigated by EPR method in the temperature range 3-300 K (Figure 1). The X-band EPR signal, containing an intense and broad line that is an envelope of a fine structure of Gd^{3+} ions, is observed in the range of 0 to about 1100 mT in the whole temperature range. At low temperature the signal is asymmetrical (Figure 2a), while at temperatures above 20 K the shape of the EPR line significantly changes, becoming close to the symmetric Lorentzian (NGP 120) or Gaussian (NGP 500, NGP 700) first derivative shape (Figure 2b). The Lorentzian shape of the EPR line suggests an exchange kind of magnetic interactions as prevailing in the powder, while the Gaussian shape of the EPR line indicates dipole-dipole interactions.

In order to describe the resonance signal of Gd^{3+} ions in powder, a spin-Hamiltonian of the following form was taken into consideration:

$$H_s = \mu_B BgS + D[S_z^2 - \frac{1}{3}S(S+1)] + E(S_x^2 - S_y^2) + \sum B_q^k O_q^k \qquad (1)$$

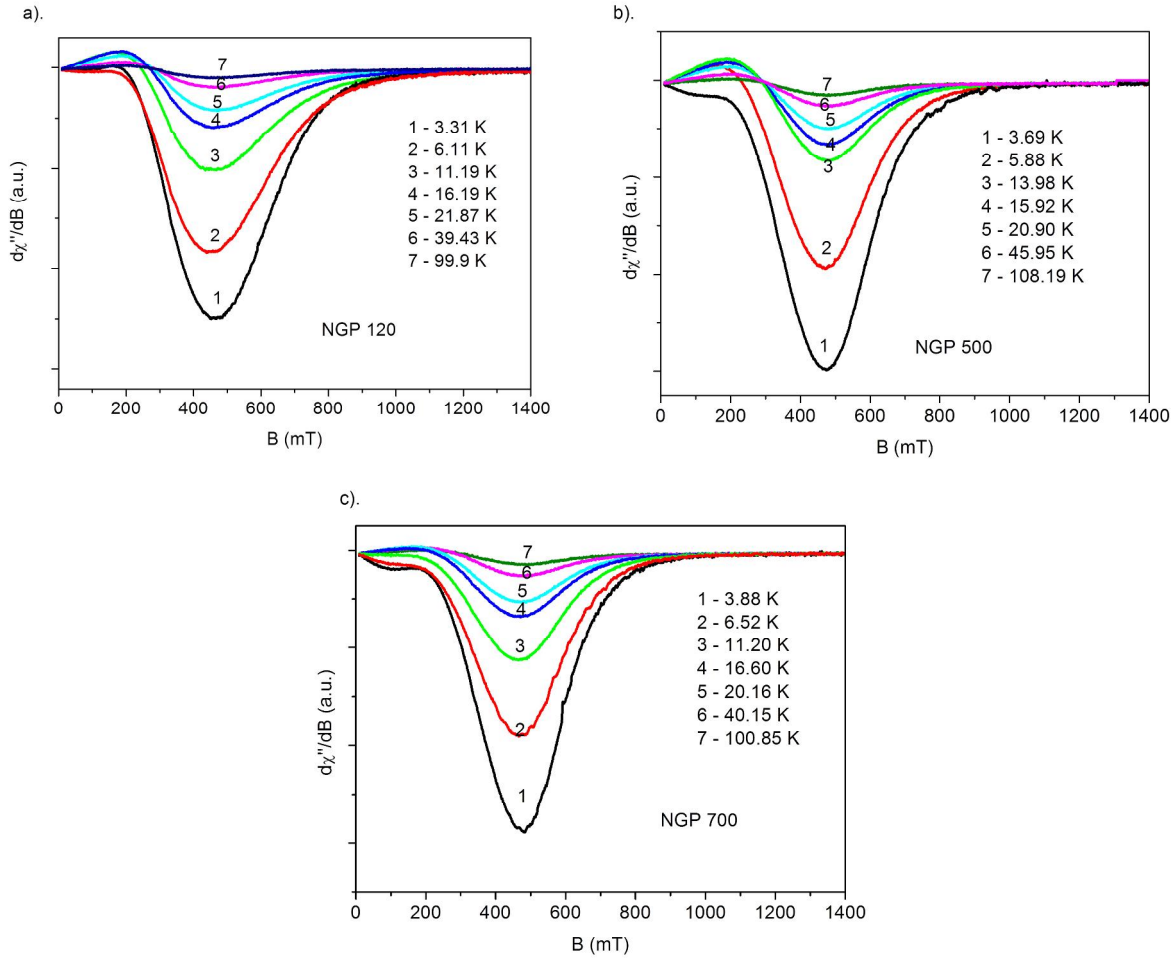

Figure 1. Temperature dependence of the EPR spectra of the $Na_3Gd(PO_4)_2$ powder calcined at 120, 500 and 700°C: (a) NGP 120, (b) NGP 500 and (c) NGP 700 samples; hydrothermal method.

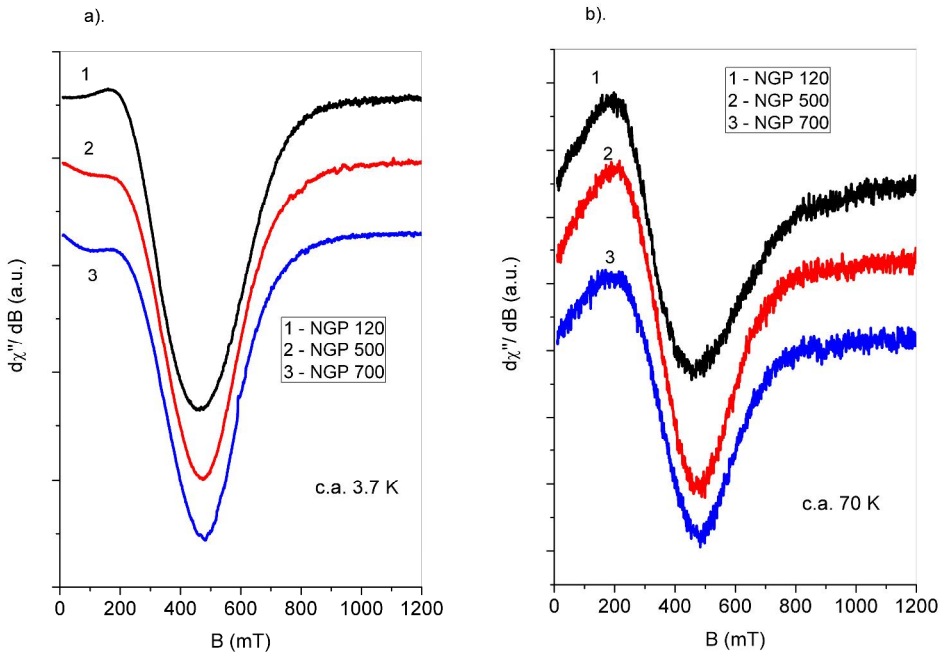

Figure 2. EPR signals of the three investigated samples at temperature 3.7 K (a) and 70 K (b).

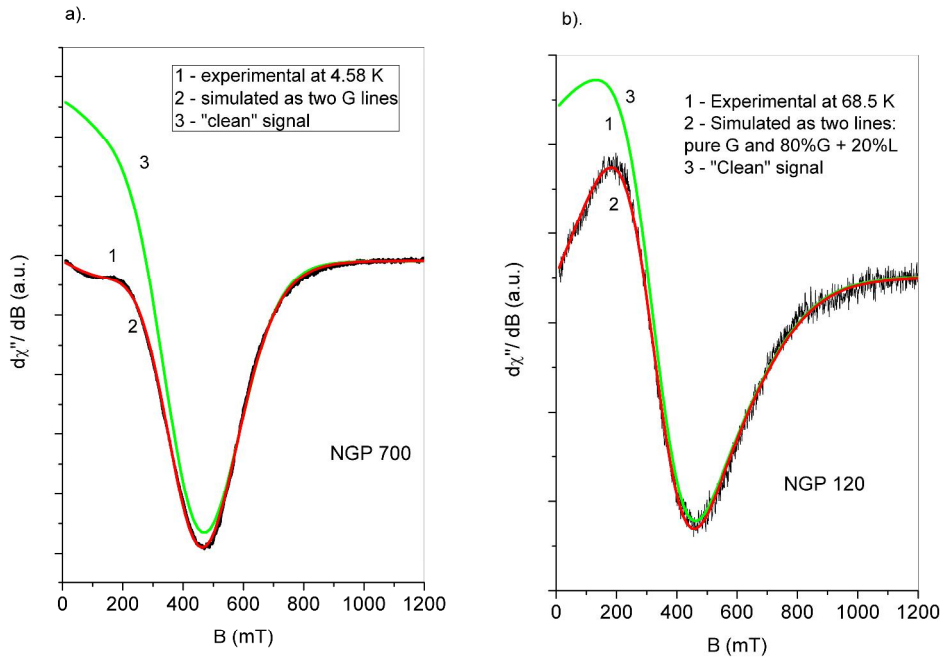

Figure 3. Two examples of the EPR signal treatment, including: simulation of the experimental signal (1) as two symmetric lines with a negative part of magnetic field (2) and separation of clean resonance signal without negative magnetic field components (3) : (a) NGP 700, (b) NGP 120.

where: the first term of the equation is a Zeeman term, the second and the third one represent the second order Steven's terms known as zero-field splitting terms, described by axial symmetry parameter *D* and rhombic distortion parameter *E*. The last term of the equation contains other Steven's parameters, of the 4-th and 6-th order, justified in the case of the total spin S= 7/2.

An analysis of the registered EPR signal by using Eq. 1 is complex. Due to a large width of the line an additional component of the resonance process, i.e. "negative" magnetic field circular component, should be taken into account. The negative component indicates readiness of some amount of spins to take part in resonance even when magnetic field is inversely directed. As used by us EPR/NMR [11] simulating program was calibrated on the mode, where negative magnetic components are not included, we treated all the resonance lines in a specific manner. The experimental signal (marked as 1 – see Figure 3) was simulated with both Gaussian and mixed Lorentzian-Gaussian lines, including physically reasonable negative magnetic components (marked as 2).

The results of the simulation seem to be very satisfying, as it is presented in Figures 3 showing EPR lines measured at different temperatures for two of the above powders. The next step of the EPR signal treatment was separation of a "clean" resonance signal (marked as 3), without negative components (upper lines in Figure 3). The "clean" signal prepared in such a way was ready for simulation process using Eq. 1 and EPR/NMR program. Several results of such a simulation are presented in Figure 4. The simulation allowed us to calculate parameters of a spin Hamiltonian. Some of them are presented in Figure 5 as a function of temperature.

Due to large width of the line, the 4-th and 6-th order Steven's terms were not calculated in our case. Some discrepancy between the observed at higher magnetic field experimental and simulated lines indicates an imperfection of the used method, but general conclusions seem to be correct and they are as follows:

1. The simulation proposed by us is quite satisfying at temperature above c.a. 15 K for all three samples, which means, that below this temperature some additional components of the EPR signal should be taken into account.
2. The shape of the resonance line is of Lorentzian type for NGP 120 and Gaussian type for NGP 500 and NGP 700 samples.
3. Relation between *D* and *E* parameters from Eq. 1 fulfills the condition E/D= 1/3, which means that the local symmetry around gadolinium centers is strongly distorted from an axial symmetry.
4. *D* parameter, expressing the strength of the crystal field around gadolinium sites is lower for NGP 120 sample and equal to $D = 470 \cdot 10^{-4}$ cm^{-1}, whereas for NGP 500 and NGP 700 samples its calculated value equals to $D = 525 \cdot 10^{-4}$ cm^{-1}; see Figure 4b (According to definition: $D = 1.5D_z$ in all the cases).
5. The resonance conditions are different for NGP 120 sample (higher *g* values) from those for the other NGP 500 and NGP 700 samples (lower *g* values); see Figure 5a.
6. The 4-th and 6-th order Steven's terms were also taken into consideration, but according to our attempts, the shape of the simulated line was improved only when B_0^4 and B_0^6 terms were taken into account. Unfortunately, due to the large width of the simulated lines the values of B_0^4 and B_0^6 are inconsistent and we decided not to present them here.

In Figure 6 we present the results of the second of two ways to describe properties of the investigated powders, mentioned in the beginning of the paper, that is temperature dependence of the resonance line positions calculated for all three samples.

As it can be seen, the conclusion drawn from the temperature dependence of the resonance line positions and analysis of the lineshape (using EPR/NMR simulation) is that they are very close to each other. Some variations of the resonance line positions, *g*, are observed. These variations could be attributed to a specific contribution of the internal magnetic fields arising from the thermally fluctuating magnetic moments that change resonance conditions. It can be confirmed having a look at the dependence of the χ_{EPR}*T product versus temperature (Figure 7). In the range of large variation in the *g* value (below 30 K) some anomaly in the values of the product, which is proportional to a square of magnetic field, is observed. The value of the magnetic moment decreases starting from NGP 120 powder to NGP 700 powder. Outside the range a

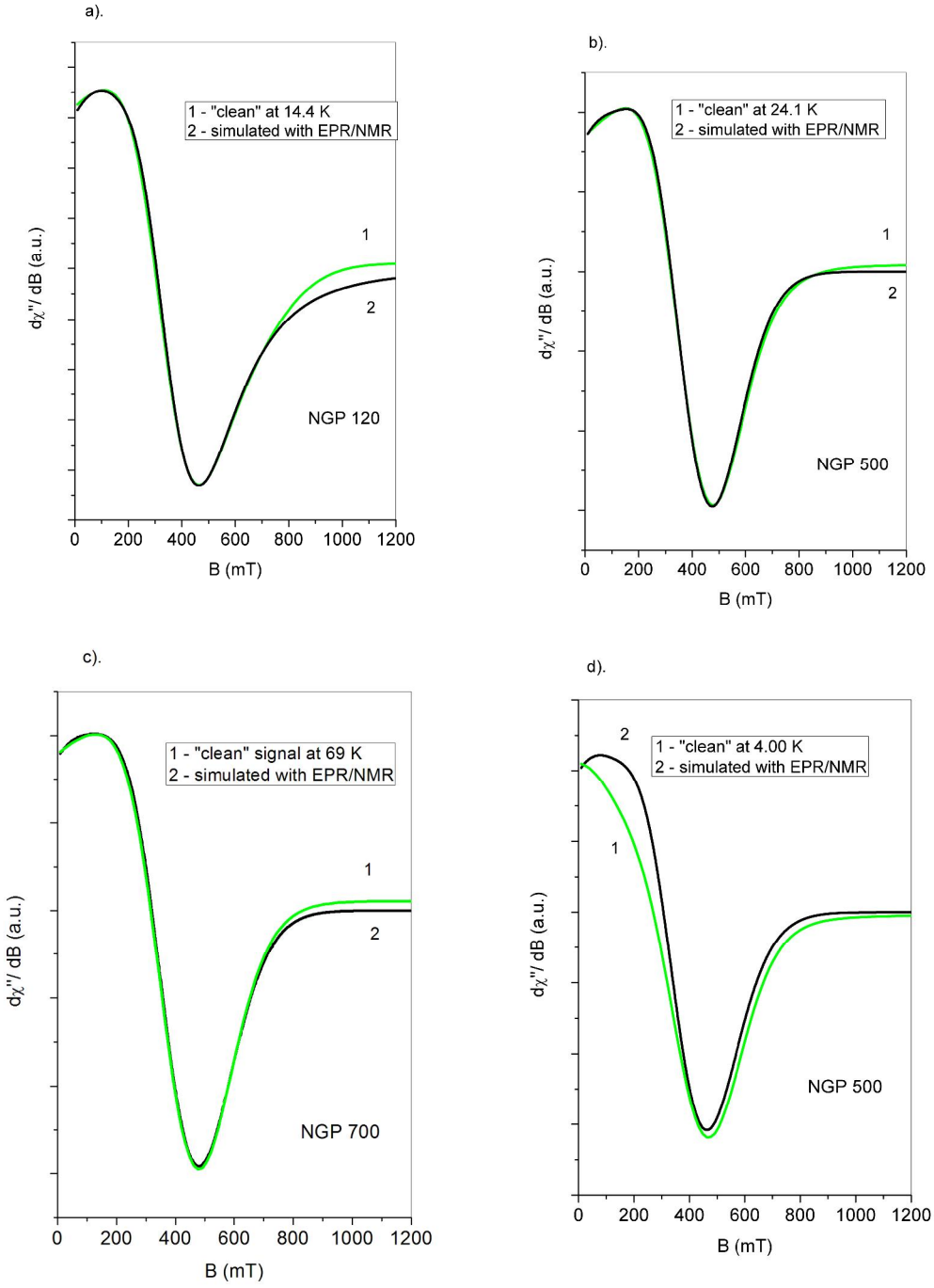

Figure 4. Examples of the resonance line simulation using Eq. 1.

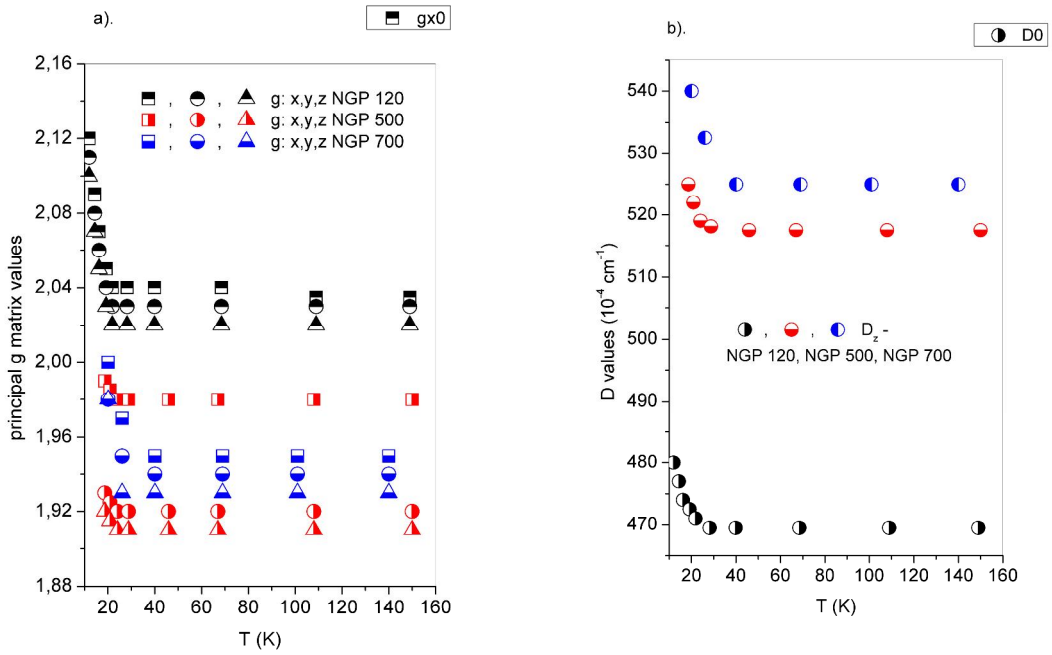

Figure 5. Temperature dependence of the spin-Hamiltonian parameters. (D= 1.5 D_z, E= 0.5 D_z); hydrothermal method.

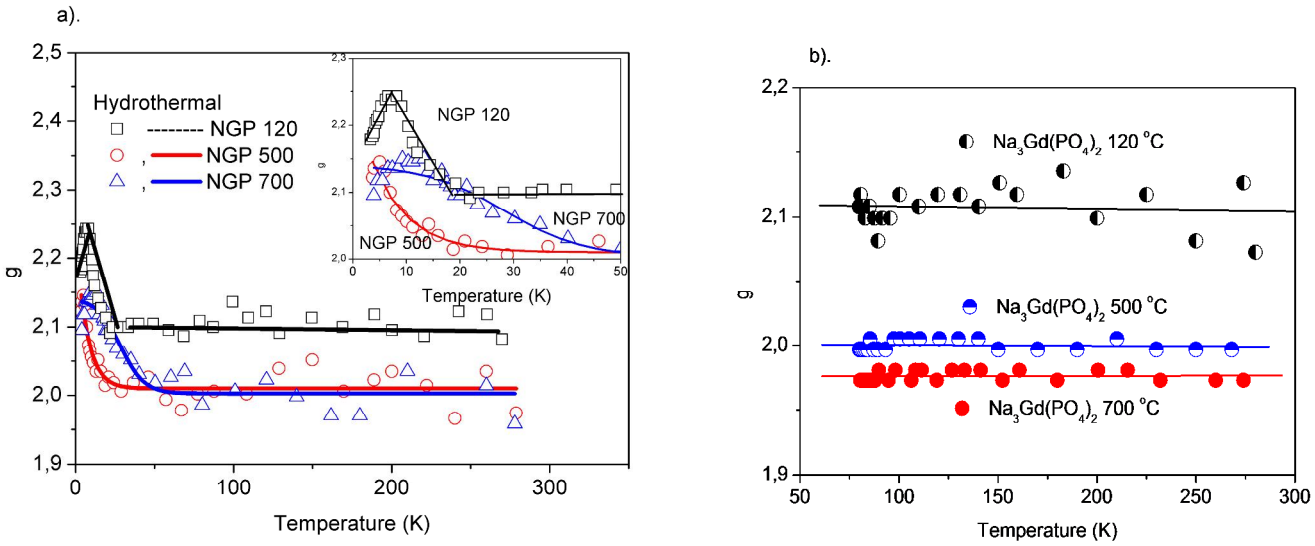

Figure 6. Temperature dependence of the resonance line positions calculated for all the three samples from: (a) helium measurements, (b) nitrogen measurements; hydrothermal method.

continuous increase in the magnetic moment with increasing temperature can be observed for all the investigated samples, which suggests an antiferromagnetic type of magnetic interactions in this temperature range.

Between 10 and 30 K, ferromagnetic like interaction can be recognized. Such a modification of the magnetic properties with temperature is found to be characteristic for all the powders. Nevertheless, they differ by a strength of magnetic interactions and *g*-factor (see Figure 6b), so they seem to have various structures. Decreasing value of *g*-factor with increasing temperature from NGP 120 to NGP 700 suggests better ordering of Gd^{3+} ions in $Na_3Gd(PO_4)_2$ powder calcined at higher temperature. The conclusion is confirmed by the value of Curie-Weiss temperature, Θ_{cw}, which is proportional to a strength of magnetic interactions. It was derived from a fitting of the Curie Weiss relation to EPR susceptibility, χ_{EPR}, calculated as a double integral of the registered EPR spectra:

$$\chi_{EPR}=C/(T-\Theta_{cw}) \quad (2)$$

where C – Curie-Weiss constant, Θ_{cw} – Curie-Weiss temperature, T – temperature.

As it can be seen from Figure 8, the Curie-Weiss temperature of $Na_3Gd(PO_4)_2$ compound decreases from NGP 120 (-1.90 K) to NGP 700

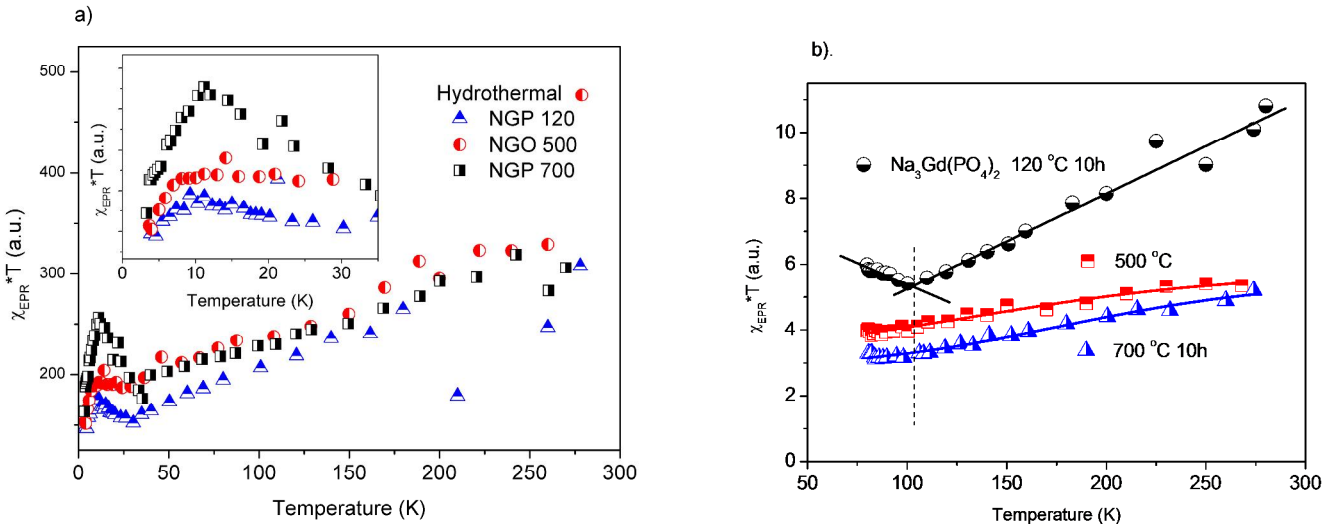

Figure 7. The χ_{EPR}*T product vs. temperature calculated for $Na_3Gd(PO_4)_2$ from: (a) helium measurements, (b) nitrogen measurements; hydrothermal method.

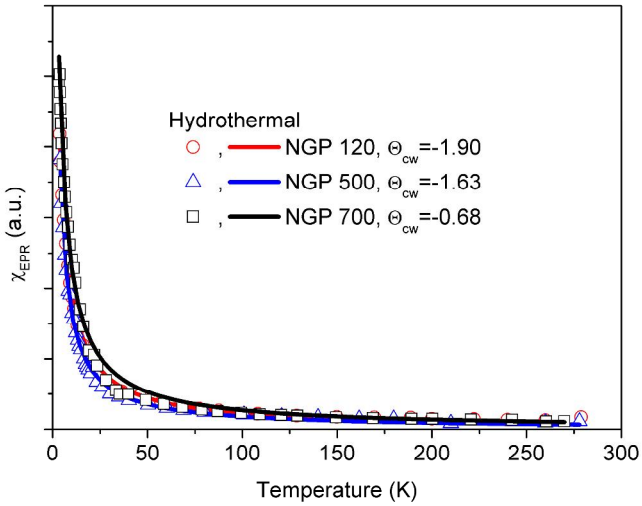

Figure 8. EPR susceptibility vs. temperature for pure $Na_3Gd(PO_4)_2$ compounds; hydrothermal method.

(-0.86 K), indicating lowering of magnetic interactions with increasing calcination temperature.

3.2. $Na_3Gd(PO_4)_2$:Yb^{3+} 5at.% powders obtained by hydrothermal method

The EPR spectra of $Na_3Gd(PO_4)_2$ powders doped with Yb (5at.%), obtained by hydrothermal method and calcined at the same conditions as the pure ones (NGPYb 120, NGPYb 500 and NGPYb 700), show very similar irregularities in temperature dependences of resonance line positions (Figure 9), the product of EPR susceptibility and temperature (Figure 10), and EPR susceptibility (Figure 11) as those of pure NGP powders (Figures 6, 7, 8, respectively) . We were not able to recognize EPR signals from ytterbium ions.

Excluding temperatures below 15 K, all the investigated doped compounds revealed low antiferromagnetic interactions (Figure 10) increasing with an increase of calcination temperature, contrary to pure NGP powders. Decreasing *g*-factor with increasing temperature indicates higher ordering of gadolinium ions. Another difference can be found in a position of the maximum of the observed irregularities, which is shifted towards half as high temperature for Yb^{3+} doped samples.

3.3. $Na_3Y(PO_4)_2$:Yb^{3+} 5at.% powders obtained by hydrothermal method

To know the EPR line-shape and thus local symmetry of the ytterbium ions in the analyzed phosphate powders, we investigated $Na_3Y(PO_4)_2$:Yb^{3+} 5at.% samples prepared in the same way as those previously described. As it can be seen in Figure 12, ytterbium ions substitute $Na_3Y(PO_4)_2$ powder at different sites. So, calcination at 120, 500 and 700°C may lead to different structures of NYPYb orthophosphates. The *g*-factors decrease with calcination temperature increase, although they fulfill the relation: $g_x=g_y=g_z$, which indicates the same type of trigonal symmetry of the compounds. Dominating interactions are of a weak antiferromagnetic–type. The Curie-Weiss temperature, Θ_{cw}, decreases with increasing calcination temperature from -2.57 K for 120°C. Ytterbium ions are involved in Zeeman, quadruple and hyperfine interactions. The latter, increasing with increasing calcination temperature, indicates lowering of the crystal symmetry that may be generally trigonal (Figure12 d, e, f – blue line) with addition of tetragonal or monoclinic (Figure 12 e, f – red line). The ytterbium ion at low symmetry reveals a strong anisotropy.

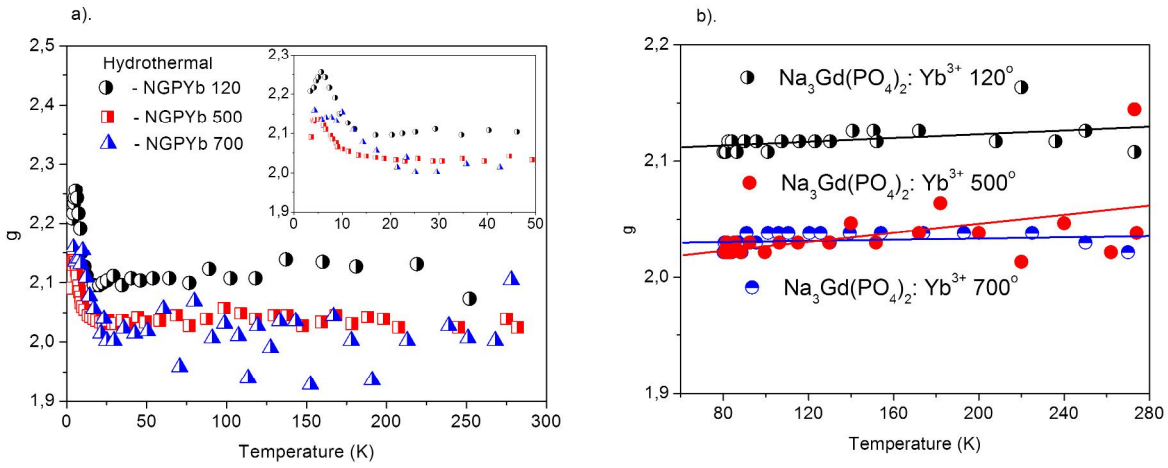

Figure 9. Temperature dependence of the resonance line positions calculated for all the three ytterbium doped samples from: (a) helium measurements, (b) nitrogen measurements; hydrothermal method.

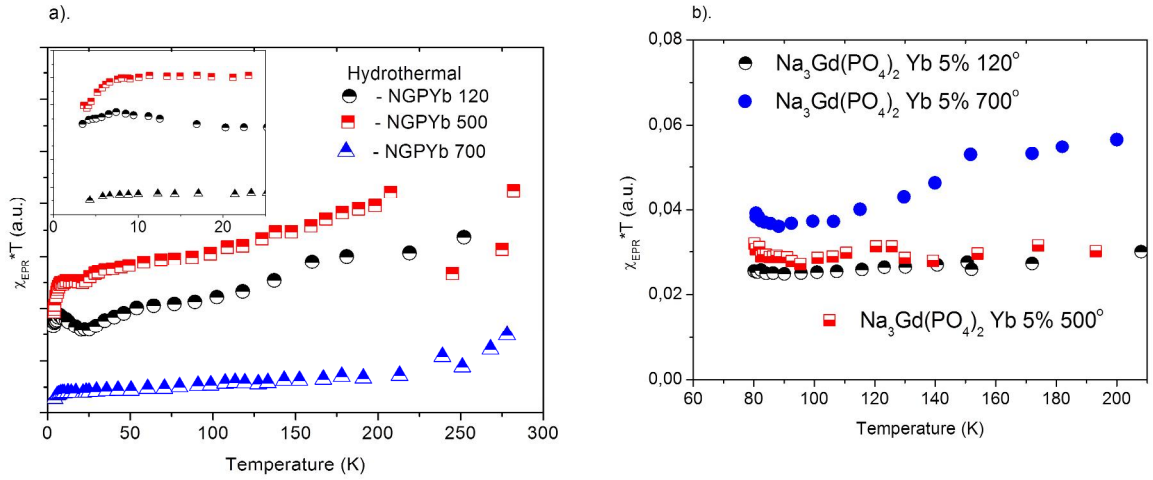

Figure 10. The χ_{EPR}*T product vs. temperature calculated for the $Na_3Gd(PO_4)_2$:Yb (5at.%) powder from: (a) helium measurements, (b) nitrogen measurements; hydrothermal method.

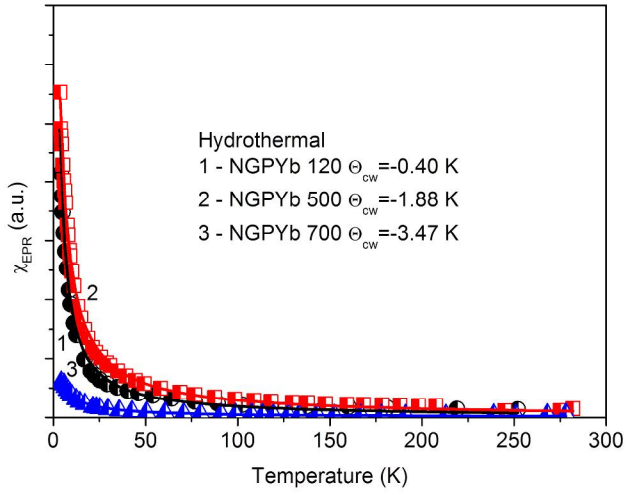

Figure 11. EPR susceptibility vs. temperature for the $Na_3Gd(PO_4)_2$ powders doped with Yb^{3+}; hydrothermal method.

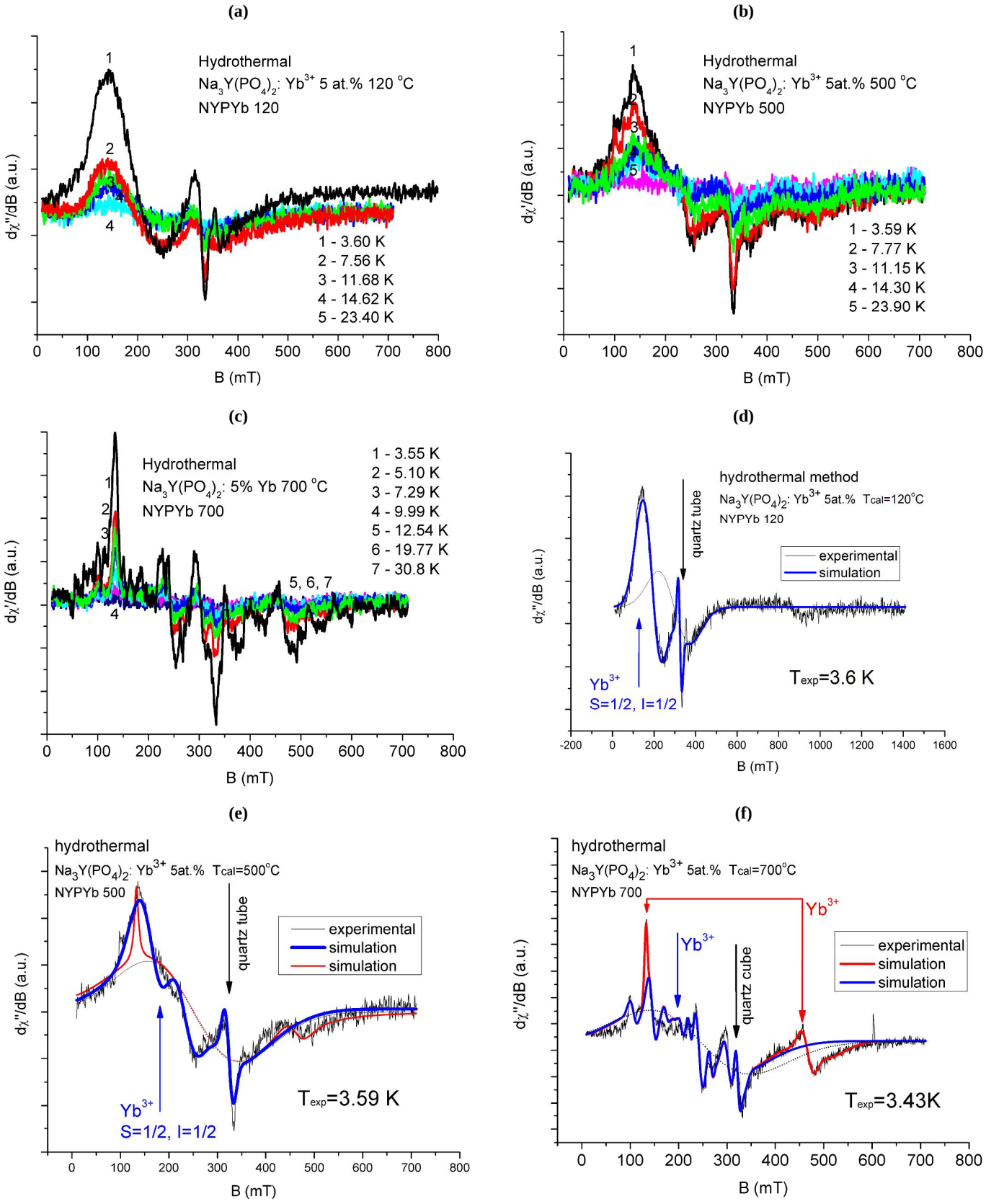

Figure 12. EPR spectra of $Na_3Y(PO_4)_2$:Yb^{3+} 5at.% orthophosphates calcined at (a) 120 °C (NYPYb 120), (b) 500 °C (NYPYb 500) and (c) 700 °C (NYPYb 700) for several temperature values, and, EPR/NMR simulation of the spectra: (d) T=3.6 K, (e) T=3.59 K and (f) T=3.43 K, respectively; hydrothermal method.

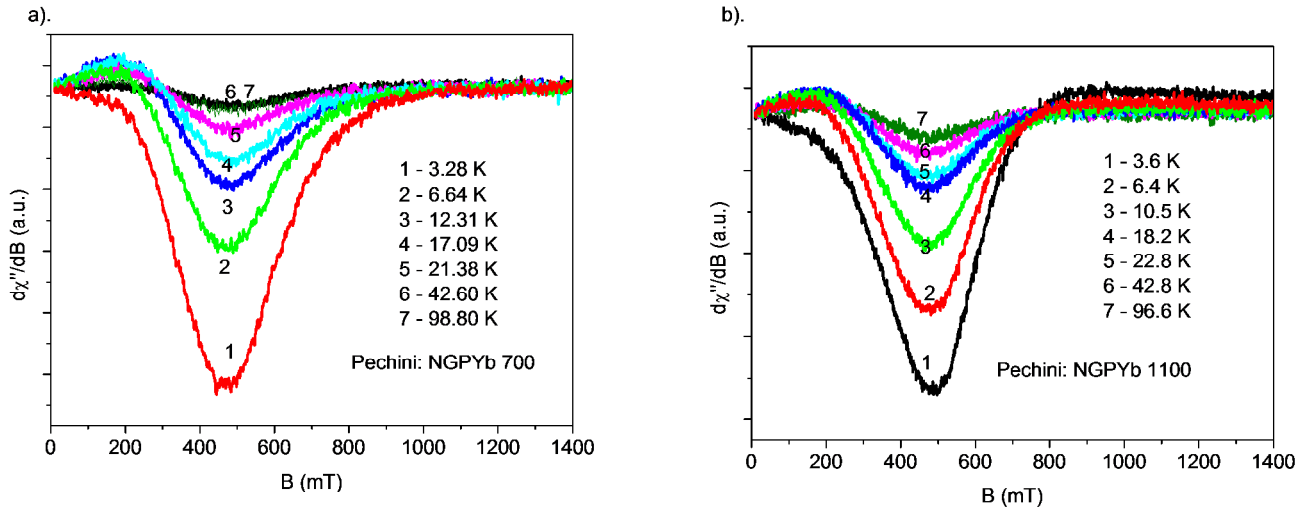

Figure 13. EPR spectra of the NGPYb 700 and NGPYb 1100 powders; Pechini method.

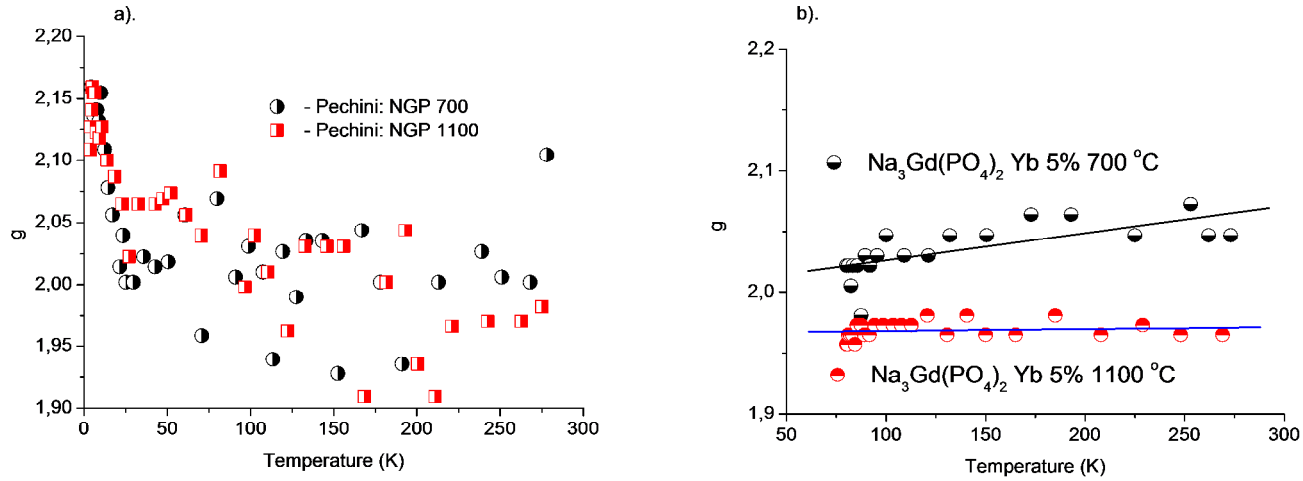

Figure 14. Temperature dependence of the resonance line positions calculated for the two samples NGP 700 and NGP 1100 from: (a) helium measurements, (b) nitrogen measurements; Pechini method.

3.4. $Na_3Gd(PO_4)_2:Yb^{3+}$ 5 at.% powders obtained by Pechini method

The EPR spectra of the $Na_3Gd(PO_4)_2$ powders doped with ytterbium 5 at.%, obtained by Pechini method, calcined at 700 and 1100 ^oC (NGP 700 and NGP 1100) are presented in Figure 13.

As it can be seen, the EPR spectra of the NGP powders doped with the same content of Yb as the compounds obtained by hydrothermal method, differ only slightly from each other, showing lack of the components giving the EPR signal in negative magnetic fields. The *g*-factor dependence v. s. temperature shows the presence of internal magnetic fields (Figure 14), but they only slightly influence overall magnetic interactions, changing the strength of antiferromagnetic interactions but not the type (Figure 15). From Figure 16 one can see that Curie-Weiss relation is fulfilled only below 100 K and shows negative values of the Curie-Weiss temperature. On increase of calcination temperature, the strength of antiferromagnetic interactions increases.

3.5. $Na_3La(PO_4)_2:Yb^{3+}$ 5at.% and $Na_3Y(PO_4)_2:Yb^{3+}$ 5at.% obtained by Pechini method

To know the shape of EPR spectra of ytterbium ions in the analyzed orthophosphate compounds obtained by Pechini method, we investigated NLPYb and NYPYb samples calcined at 700^oC and NLPYb calcined at 1150^oC. The EPR spectra of the samples are presented in Figure 17 a, c and b, respectively.

Calcination of the NLPYb powder at 700 and 1150 ^oC does not change the shape of the EPR spectra. The Θ_{cw} decreases with an increase of calcination temperature from 2.12 K indicating prevailing ferromagnetic interactions between Yb^{3+} ions. The calcination does not lead to a change in the powder structure. As it can be seen, the EPR spectra (Figure 17) reveal a different site symmetry of ytterbium ions for the second of the orthophosphates (NYPYb, Θ_{cw} =-2.16 K), similar to that of the obtained by hydrothermal method NYPYb powders (see Figure 18). Spin Hamiltonian parameters are the same as those gathered in Table 3.

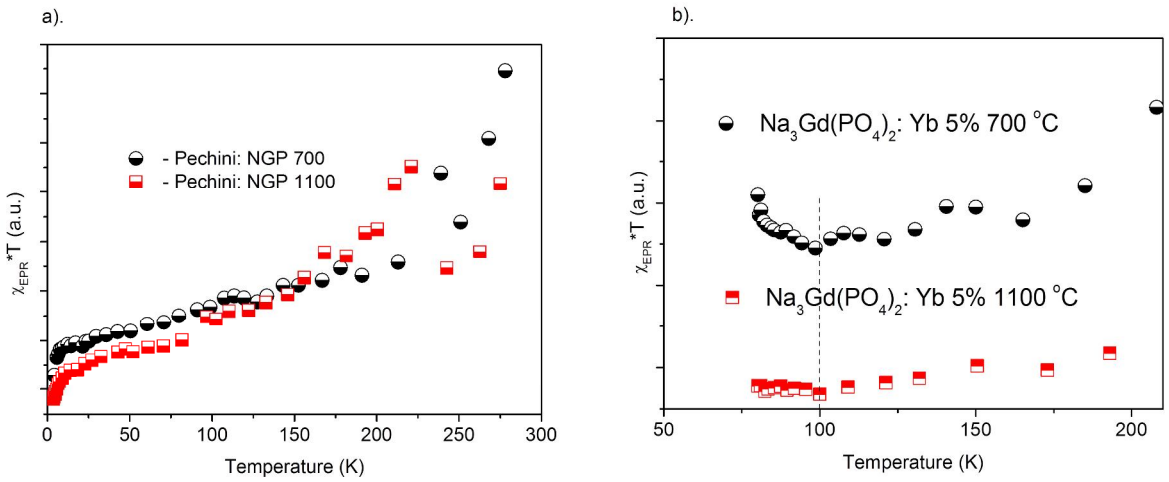

Figure 15. The χ_{EPR}*T product vs. temperature calculated for the $Na_3Gd(PO_4)_2$:Yb (5at.%) powder (NGPYb) from: (a) helium measurements, (b) nitrogen measurements; Pechini method

Table 3. Spin Hamiltonian parameters calculated using the shape of the measured EPR spectra and EPR/NMR program for NYPYb 120, 500 and 700 compounds. The elements of hyperfine (A) and quadrupole (P) matrices are given in mT units.

NYPYb 120			**NYPYb 500**			**NYPYb 700**			
3.37	0	0	3.16	0	0	3.21	0	0	g-matrix, S=1/2
0	3.37	0	0	3.16	0	0	3.21	0	
0	0	3.37	0	0	3.16	0	0	3.21	
9.0	0	0	9.0	0	0	19.0	0	0	P – matrix, I=5/2
0	19.0	0	0	19.0	0	0	9.0	0	
0	0	-18.0	0	0	-18.0	0	0	-18.0	
30.0	0	0	34.0	0	0	36.05	0	0	A_1 – matrix, I=5/2
0	30.0	0	0	34.0	0	0	36.05	0	
0	0	30.0	0	0	34.0	0	0	36.05	
60.0	0	0	100.0	0	0	154.8	0	0	A_2 – matrix, I=1/2
0	60.0	0	0	100.0	0	0	154.8	0	
0	0	60.0	0	0	100.0	0	0	154.8	
						1.45	0	0	g-matrix, S=1/2
						0	1.45	0	
						0	0	5.08	
						78.2	0	0	A – matrix, I=1/2
						0	78.2	0	
						0	0	78.2	

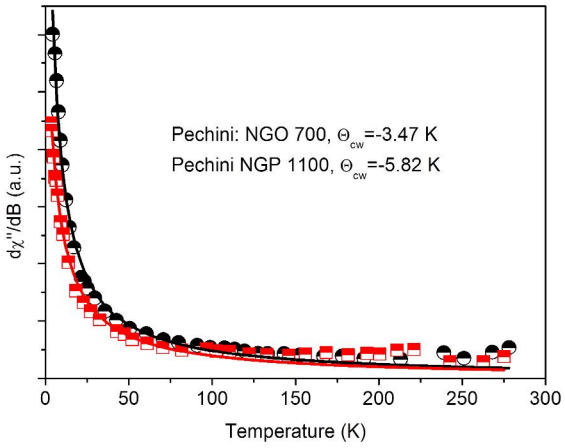

Figure 16. EPR susceptibility vs. temperature calculated for the $Na_3Gd(PO_4)_2$ powders doped with Yb^{3+} (NGPYb), Pechini method.

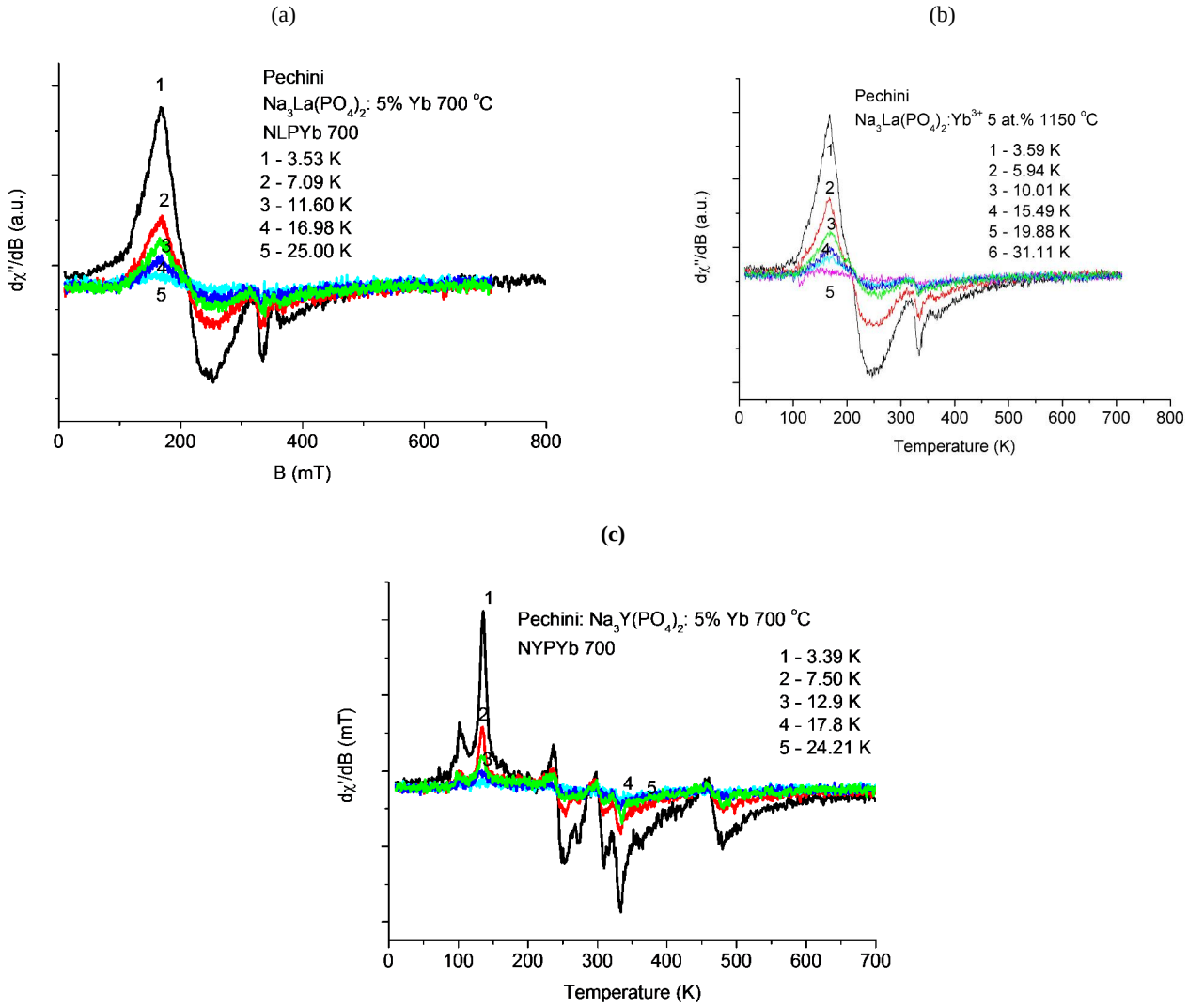

Figure 17. Temperature dependence of EPR spectra measured for the NLPYb and NYPYb samples obtained by Pechini method: (a) NLPYb 700, (b) NLPYb 1150, (c) NYPYb 700; Pechini method.

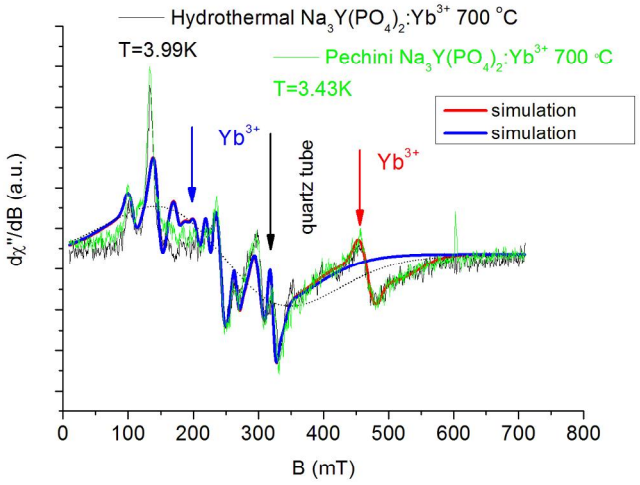

Figure 18. Comparison of the EPR/NMR simulation of the EPR spectra recorded for yttrium orthophosphates doped with ytterbium, obtained by hydrothermal and Pechini methods; T=3.99 K.

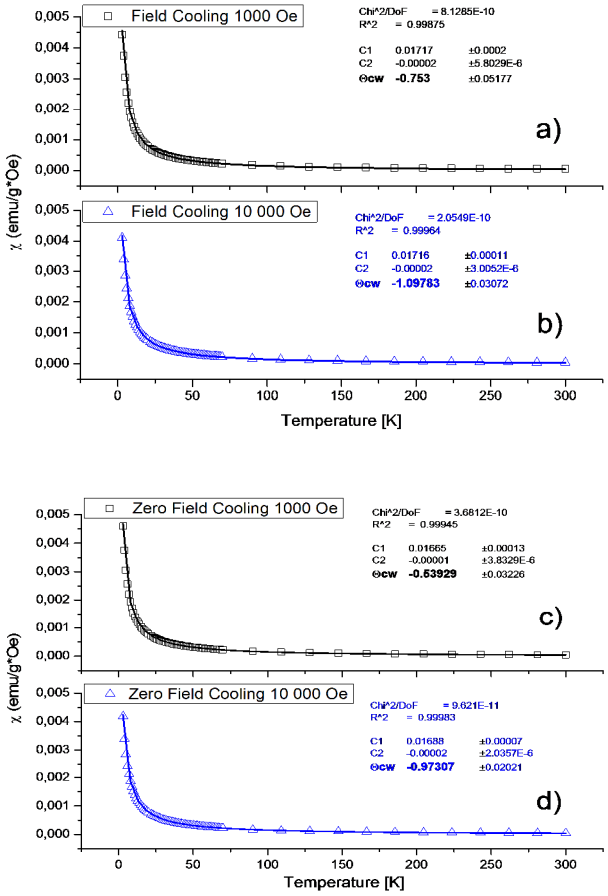

Figure 19. Magnetic susceptibility of the $Na_3Gd_{1-x}Yb_x(PO_4)_2$; x=0.05, 700 °C (NGPYb 700) sample obtained by Pechini method for two magnetic fields: 1000 and 10,000 Oe and FC: (a), (b) and ZFC: (c), (d) modes. Solid lines represent fittings according to eq. 3.

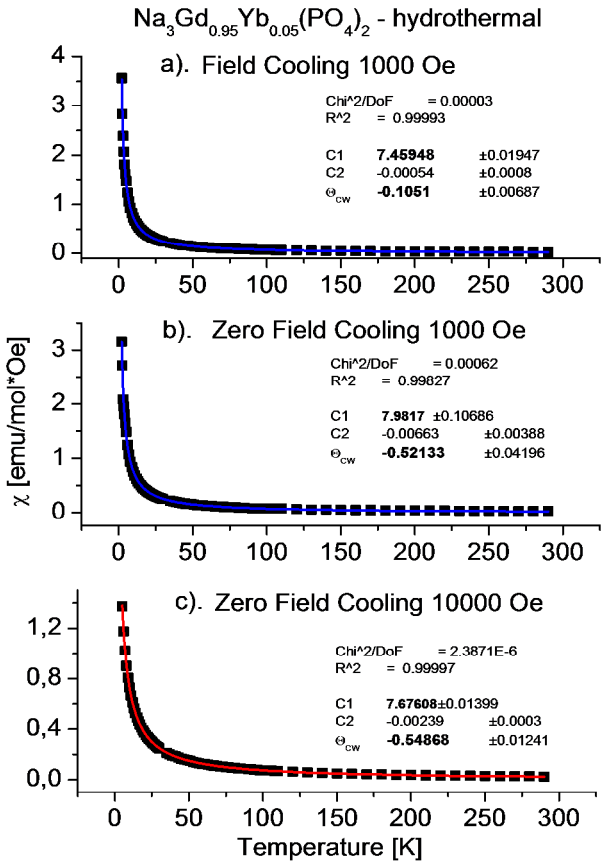

Figure 20. Magnetic susceptibility of $Na_3Gd_{1-x}Yb_x(PO_4)_2$; x=0.05, 700°C sample (NGPYb 700): (a) FC mode for 1000 Oe and (b) and (c). ZFC modes for two magnetic fields: 1000 and 10,000 Oe, as a function of temperature. Solid lines represent fittings according to eq. 3

3.6. Susceptibility measurements

Taking into account a possible influence of ytterbium ions on the structure of the orthophosphates it is reasonable to analyze magnetic susceptibility as a function of temperature for several values of magnetic field. We performed measurements of magnetic susceptibility in FC and ZFC modes of the NGPYb 700 sample obtained by Pechini method (Figure 19), and obtained NGP 700 by hydrothermal method (Figure 20) and NGPYb 700 (Figure 21) samples for two values of magnetic field: 1000 Oe and 10,000 Oe. The fittings of the results to Curie-Weiss law were conducted according to the following equation:

$$\chi_m = \frac{C_1}{T-\Theta_{cw}} + C_2\,, \qquad (3)$$

where C_1 is Curie-Weiss constant and C_2 is a parameter improving the fitting, in which the diamagnetic factor is taken into account.

There was no phase transition observed in the temperature range 4-300 K.

In the case of the sample obtained by Pechini method, the calculated values of Curie-Weiss temperatures, Θ_{cw}, are as high as -0.75 K and -1.1 in FC mode and -0.53 K and -0.97 in ZFC mode, for 1000 and 10,000 Oe, respectively, indicating lack or very weak magnetic interactions, mainly of an antiferromagnetic type. There is a very good agreement between magnetic susceptibility and EPR measurements (-0.47 K).

We calculated the theoretical value of the effective magnetic moment of the sample according to the following equation [12]:

$$\mu_{eff} = \sqrt{x\cdot {\mu_{eff\,1}}^2 + (1-x)\cdot {\mu_{eff\,2}}^2}\,, \qquad (4)$$

where x - Yb content, and, $\mu_{eff,\,1,\,2}$ - are effective magnetic moments of free ions (4.54 μ_B for Yb, and 7.94 μ_B for Gd, μ_B – Bohr magneton). As we expected that Yb^{3+} ions substitute Gd^{3+} ions, the correct stoichiometry of the investigated compounds should be described as: $Na_3Gd_{1-x}Yb_x(PO_4)_2$; x=0.05 (see caption of Figure 19). The calculated theoretical value was equal to 7.81 μ_B.

The calculations of an effective magnetic moment based on experimental data were performed using Curie-Weiss constant, C_1, according to the following relation [13]:

$$\mu_{eff} = \sqrt{\frac{3kC_1}{N}} = 2.827\cdot\sqrt{C_1}\,,\ \ \chi_m = \frac{N\cdot {\mu_{eff}}^2}{3kT} = \frac{C_1}{T}\,[\mu_B] \qquad (5)$$

where k – Boltzmann constant, N – Avogadro number, C' – Curie constant, T – temperature. With this aim we changed curves presented in Figure 19 by replacing ordinate axis from χ in emu/g*Oe to χ in emu/mol*Oe.

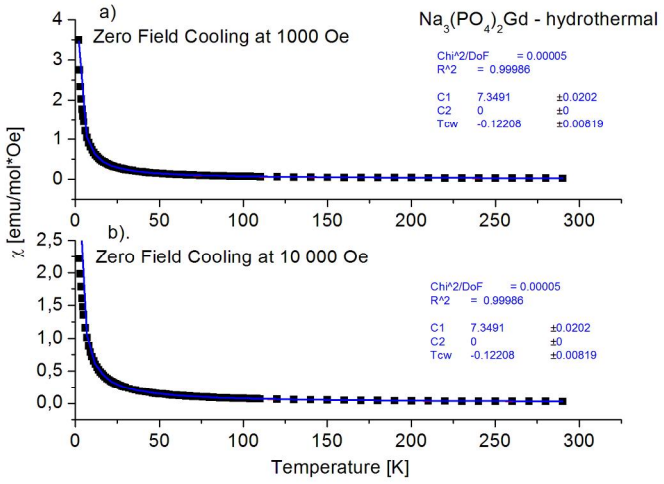

Figure 21. Magnetic susceptibility of the $Na_3Gd(PO_4)_2$ 700°C sample (NGP 700): (a) ZFC mode for 1000 Oe and (b) ZFC mode for 10,000 Oe, as a function of temperature. Solid lines represent fittings according to eq. 3

We obtained:
- in FC mode: ~7.75±0.06 μ_B for both magnetic fields 1000 and 10,000 Oe,
- in ZFC mode: 7.63±0.06μ_B and 7.68±0.06 μ_B for 1000 and 10,000 Oe, respectively.

So, the theoretical value of the effective magnetic moment, 7.81 μ_B, differs only slightly from the calculated ones obtained from the experimental data. It means that the real stoichiometry of the sample obtained by Pechini method agrees very well with the predicted one.

In the case of the NGPYb 700 sample doped with ytterbium obtained by hydrothermal method doped with ytterbium NGPYb 700 sample, (Figure 20), the calculated values of Curie-Weiss temperatures, Θ_{cw}, are as high as -0.11 K in FC mode for 1000 Oe and -0.52 K and -0.55 K in ZFC mode, for 1000 and 10,000 Oe, respectively, indicating very weak magnetic interactions, mainly of an antiferromagnetic type, similarly as in the case of Pechini sample. The theoretical value of an effective magnetic moment is the same as previously, 7.81 μ_B. The values of effective magnetic moments calculated on the basis of the experimental data (see eq. 3) are following:
- in FC mode: ~7.72±0.06 μ_B for 1000 Oe,
- in ZFC mode: 7.99±0.06 μ_B and 7.83±0.06 μ_B for 1000 and 10,000 Oe, respectively.

The above values differ only slightly from the theoretical one, 7.81 μ_B. So, the stoichiometry of the compound seems to be in a good agreement with the predicted one.

In the case of the NGP 700 sample obtained by hydrothermal method without doping (Figure 21), the calculated values of Curie-Weiss temperatures, Θ_{cw}, are as high as -0.12 K in ZFC mode, for both 1000 and 10,000 Oe, indicating very weak magnetic interactions, mainly of an antiferromagnetic type, similarly as in the case of the samples doped with Yb. The theoretical value of the effective magnetic moment is now, 7.94 μ_B. The values of effective magnetic moments calculated on the basis of the experimental data (see eq. 3) are following:
- in ZFC mode: 7.66±0.08 μ_B for both 1000 and 10,000 Oe.

The difference between theoretical value of the effective magnetic moment, 7.94 μ_B, and the presented above experimental one, suggests some deviation from stoichiometry.

4. DISCUSSION

The results of X-ray, IR and Raman measurements [8] show that applying of various calcination temperature leads to different phases of the studied compounds as well as to different compositions of the investigated samples. Similar conclusions result from the EPR measurements. As-synthesized materials can be described by the trigonal P-3m1 (D_{3d}^3, No. 162, Z = 1) symmetry corresponding to that of the high-temperature phase of bulk samples [1]. These samples are single phase. The calcination of the studied phosphates at 500 and 700 °C changes their microstructure as well as the sample composition. The samples calcined at 500 °C contain two modifications: the described above trigonal phase and the orthorhombic phase ($Pca2_1 = C_{2v}^5$) built of nano-sized crystallites. This nanophase has a structure similar to that of β-$Na_3Ce(PO_4)_2$ [14].

The subsequent calcination at 700 °C leads to disappearing of the trigonal phase. The crystals obtained by Pechini method have monoclinic C2/c (C_{2h}^6) symmetry. All the above conclusions were confirmed to some extent by EPR investigations, especially by different ordering of gadolinium ions manifesting different values of Curie-Weiss temperatures and *g*-factors. Increasing calcination temperature should transform the crystal structure towards higher symmetry due to decreasing *g*-factor. However, for the precursor samples the trigonal phase was observed, known to appear at high temperature of bulk material (above about 980°C for $Na_3Gd(PO_4)_2$), next, the sample calcined at 500°C has a structure of the middle-temperature phase of bulk crystal (orthorhombic phase between 950 and 980°C), and finally, the sample obtained at the highest temperature contains the monoclinic phase known from bulk material at room temperature. So, two phenomena compete in realizing of the phase sequence. The multiphase character of the samples disturbs the typical behaviour of nanocrystalline materials, i.e. the crystals growth with rising calcination temperature in the case of the trigonal phase and lowering of the symmetry with the increase of calcination temperature, i.e. the ‘‘inversion’’ of thermally induced sequence of phases in bulk crystal.

5. CONCLUSIONS

EPR analysis allowed to find clear differences between arrangement of gadolinium ions in pure and $Na_3Gd(PO_4)_2$ phosphates doped with ytterbium, obtained by hydrothermal and Pechini methods. We have also found clear differences between the local environment of ytterbium ions in the analyzed orthophosphates calcined at 120, 500 and 700°C (obtained by hydrothermal method) and at 700 and 1100°C (obtained by Pechini method). Magnetic susceptibility measurements confirmed the conclusions drawn from EPR measurements: dominating interactions are of an antiferromagnetic type, lack of structural and phase transitions in the temperature range under investigation. Calcination of the studied phosphates at 500, 700 and 1100°C changes their microstructure as well as the sample composition.

REFERENCES

1. M. Vlasse, C. Parent, R. Salmon, G. Le Flem, P. Hagenmuller, J. Sol. State Chem. 35 (1980) 318.
2. P. P. Melnikov, L. N. Komissarova, Koord Khimia 12 (1986) 1299.
3. S. V. Ushakov, A. Navrotsky, J M Farmer and L A Boatner, J. Mater. Res. 19 (2004) 2165.
4. V. Janovec, P. Tomaszewski, L. Richterová, Z. Kluiber, Ferroelectrics 301 (2004) 169.
5. R. Salmon, C. Parent, A. Berrada, R. Brochu, A. Daoudi, M. Vlasse, G. Le Flem, CR Acad. Sci. Paris C 280 (1975) 805–808.
6. M. Fang, W. D. Cheng, H. Zhang, D. Zhao, W. L. Zhang, S. L. Yang, J. Solid State Chem. 181 (2008) 2165–2170.

7. A. Matraszek, P. Godlewska, L. Macalik, K. Hermanowicz, J. Hanuza, I. Szczygieł, J. All. Comp. 619 (2015) 273.
8. P. Godlewska, A. Matraszek, L. Macalik, K. Hermanowicz, M. Ptak, P. E. Tomaszewski, J. Hanuza, I. Szczygieł, J. All. Comp. 628 (2015) 199.
9. A. Abragam, B. Bleaney, Electron paramagnetic resonance of transition ions, Clarendon Press, Oxford (1970).
10. G. Morin, D. Bonnin, J. Magn. Reson. 136 (1999) 176.
11. M. J. Mombourquette, J. A. Weil, D. G. McGavi, EPR-NMR User's Manual, Department of Chemistry, University of Saskatchewan, Saskatoon (1999).
12. N. N. Lubinskii, L. A. Bashkirov, A. I. Galyas, S. V. Shevchenko, G. S. Petrov, I M Sirota, Inorg. Chem. 44 (2008) 1015.
13. J. H. van Vleck, Physics (1977) 353.
14. O. G. Karpov, D. Yu. Puchcharovskii, A. P. Khoymakov, E. A. Pobedimskaya, N. V. Belov, Kristallografiya+ 25 (1980) 650.

Cite this article as:

S. M. Kaczmarek *et al.*: EPR and magnetic studies of sub-microcrystalline pure and Yb doped $Na_3B(PO_4)_2$ (B=Y, La, Gd) orthophosphates synthesized by hydrothermal and Pechini method. Sci. Adv. Today 2 (2016) 25243.